Identification of Novel Tumor Microenvironment-Related Long Non-coding RNAs to Predict the Prognosis for Hepatocellular Carcinoma

Shenglan Huang
Nanchang University Second Affiliated Hospital
Jian Zhang
Nanchang University Second Affiliated Hospital
Dan Li
Nanchang University Second Affiliated Hospital
Xiaolan Lai
Ningde Normal University
Lingling Zhuang
Nanchang University Second Affiliated Hospital
Jianbing Wu (Ndefy93008@ncu.edu.cn)
Nanchang University Second Affiliated Hospital https://orcid.org/0000-0003-3405-7913

Research article

Keywords: hepatocellular carcinoma, tumor microenvironment, lncRNA, prognostic signature, immune checkpoint inhibitors.

Posted Date: September 30th, 2021

DOI: https://doi.org/10.21203/rs.3.rs-877901/v1

Abstract

Introduction: Hepatocellular carcinoma (HCC) is one of the most common malignant tumors with poor prognosis. Tumor microenvironment (TME) plays a vital role in the tumor progression of HCC. Thus, we aimed to analyze the association of TME with HCC prognosis, and construct an TME-related lncRNAs signature for predicting the prognosis of HCC patients.

Methods: We firstly assessed the stromal/immune /Estimate scores within the HCC microenvironment using the ESTIMATE algorithm based on TCGA database, and its associations with survival and clinicopathological parameters were also analyzed. Then, different expression lncRNAs were filtered out according to immune/stromal scores. Cox regression was performed to built an TME-related lncRNAs risk signature. Kaplan–Meier analysis was carried out to explored the prognostic values of the risk signature. Furthermore, we explored the biological functions and immune microenvironment feathers in high- and low risk groups. Lastly, we probed the association of the risk signature with the treatment responses to immune checkpoint inhibitors (ICIs) in HCC by comparing the immunophenoscore (IPS).

Results: Stromal/immune /Estimate scores of HCC patients were obtained based on the ESTIMATE algorithm. The Kaplan-Meier curve analysis showed the high stromal/immune/ Estimate scores were significantly associated with better prognosis of the HCC patients. Then, six TME-related lncRNAs were screened for constructing the prognosis model. Kaplan-Meier survival curves suggested that HCC patients in high-risk group had worse prognosis than those with low-risk. ROC curve and Cox regression analyses demonstrated the signature could predict HCC survival exactly and independently. Function enrichment analysis revealed that some tumor- and immune-related pathways associated with HCC tumorigenesis and progression might be activated in high-risk group. We also discovered that some immune cells, which were beneficial to enhance immune responses towards cancer, were remarkably upregulated in low-risk group. Besides, there was closely correlation of immune checkmate inhibitors (ICIs) with the risk signature and the signature can be used to predict treatment response of ICIs.

Conclusions: We analyzed the impact of the tumor microenvironment scores on the prognosis of patients with HCC. A novel TME-related prognostic risk signature was established, which may improve prognostic predictive accuracy and guide individualized immunotherapy for HCC patients.

Introduction

Liver cancer is one of the commonest malignant cancers and ranks as the fourth leading cause of cancer-related mortality worldwide[1]. Statistically, more than 800 thousand new cases were found who suffering from primary liver cancer annually, and the number of liver cancer related deaths approximately reached 780 thousand. Hepatocellular carcinoma (HCC) is the most common liver cancer, accounting for 75–85% of primary liver cancer[2, 3]. Currently, potentially curative treatments, including surgical resection, radiofrequency ablation (RFA), and liver transplantation, can be applied to early-stage patients[4]. Nevertheless, the majority of HCC patients have lost the opportunity of hepatectomy when

they are diagnosed, which results in a poor prognosis with a 5-year survival rate is no more than 18%[4, 5]. In recent years, immunotherapy has become a research hotspot for advanced HCC, including immune checkpoint blockade, adoptive cell therapy, oncolytic virus, and oncolytic bacteria. Among them, immune-checkpoint inhibitor-based therapies represented by anti-CTLA4, anti-PD1, and anti-PD-L1 have achieved a certain clinical efficacy in HCC[6]. The clinical studies of Checkmate-040[7]and Keynote-224[8]have evaluated the efficacy and safety of anti-PD1 in the advanced HCC, and the results demonstrated median survival time of nivolumab and pembrolizumab were 15.6 months and 12.9 months, respectively. However, PD1 and/or PD-L1 inhibition is only beneficial in ~ 20% of HCC patients, and there are still a considerable number of patients who cannot respond to immunotherapy[9]. Such poor objective response rate mainly due to drug resistance, high heterogeneity, and complex regulation mechanism of tumor microenvironment (TME) in HCC patients. Thus, it is urgently needed to search highly sensitive and specific prognostic biomarkers for predicting survival and clinical outcome of immunotherapy in HCC patients.

The tumor microenvironment (TME) of HCC is mainly composed of tumor cells, stromal cells, immune cells, cytokines, and the extracellular matrix, which plays crucial role in tumorigenesis and progression, immune escape, and therapeutic resistance[10]. Compared with other solid tumors, the immune microenvironment of HCC shows stronger immunosuppression. A large number of immune cell subtypes (i.e. tumor-associated macrophages, tumor-associated neutrophils, myeloid-derived suppressor cells) and other regulatory mechanisms contribute to the progress of HCC[10]. For example, increasing studies have confirmed the monocytes would be domesticated into M2 macrophages by the tumor microenvironment and secretes anti-inflammatory cytokines such as IL-8, IL-10 and TGF- β, which participate in angiogenesis, anti-inflammatory, matrix remodeling, inducing apoptosis of CD8 + T cells, inhibiting Th1 immune response, and reshaping TME, so as to promote tumor growth, invasion and metastasis[11, 12]. Besides, Tregs/CTLs ratio in TME reflect the local immune balance state of HCC, the increase of Tregs are often associated with an immunosuppressive tumor microenvironment and poor prognosis[13]. Therefore, a better understanding of cell components and immune-related factors in the HCC microenvironment is essential for identifying new prognostic and therapeutic targets, which consequently predict the response and efficacy of immunotherapy.

Long non-coding RNAs (lncRNAs), which accounts for 80 to 90% of all ncRNAs and structurally contains more than 200 nucleotides (nt) in length, play indispensable roles in the tumorigenesis and progression. Hence, lncRNAs are widely applied in tumor biomarkers for early diagnosis, prognosis, potential therapeutic target and drug resistance[14–16]. Notably, lncRNAs also have been found to be the key players in regulating cancer immunity, including antigen release, antigen presentation, immune cell priming and T cell activation, and immune cell migration[17]. For example, it was reported that lncRNA NNT-AS1 impaired CD4 T cell infiltration via activation of the TGF-β signaling pathway in HCC[18]. lncRNAs regulate pro-inflammatory cytokines level of IFN-γ and TNF-α, which are crucial to antigen presentation[19]. LncRNA-cox2 mediates both the activation and repression of immune genes, and inhibits the expression of chemokines (Ccl5, Cx3c11) and cytokine receptors (Ccrl)[20]. lncRNA AFAP1-AS1 have been found to regulate PD-1/PD-L1 signaling and upregulates the expression of PD1 in TME of

nasopharyngeal carcinoma[21]. Similarly, lncRNA UCA1 promotes proliferation, migration, immune escape of cancer cells in gastric cancer, induces a higher PD-L1 expression and decreases the secretion of IFN-γ via restraining miR-26a/b, miR-193a and miR-214 expression[22]. These findings pointed out that lncRNAs are involved in the regulation of TME, demonstrating that some certain lncRNAs may be excellent predictors or targets for immunotherapy.

In this study, we firstly assessed the immune/stromal/Estimate scores within the HCC microenvironment using the ESTIMATE algorithm based on TCGA database, and its associations with survival and clinicopathological parameters were also analyzed. Then we filtered out intersecting TME-related lncRNAs and explored its prognostic values in HCC patients. In addition, functional enrichment analysis was conducted to investigate the potential mechanism. Additionally, the relationship of lncRNAs signature with specific tumor immune microenvironment features was probed in more depth. Meanwhile, we explored the associations between these predictors and immune checkpoint blockade–related genes, and applied those TME-related lncRNAs to predict treatment response to immune checkpoint inhibitors (ICIs) in HCC. The diagram of this study was shown in Fig. 1.

Materials And Methods

Data Collection and Processing

The RNA sequencing data of 374 tumor samples and 50 normal samples was obtained from the Cancer Genome Atlas (TCGA) Genomic Data Commons (GDC) database (https://portal.gdc.cancer.gov/). The genes were commented and sorted to14142 lncRNAs and 19659 protein-coding genes according to the ENSEMBL database http://asia.ensembl.org/index. html). LncRNAs whose average expression value was less “0.1” were discarded, final 3848 lncRNAs were retained for subsequent differential analysis. The relevant clinicopathological information were downloaded from the UCSC XENA database (http://xena.ucsc.edu/), which incorporated gender, age, histological grade, clinical stage, TNM stage, and survival status, survival time (including Overall Survival, Progression Free Survival, and Disease Free Survival). After removing the patients with 0 day follow-up time, the remaining 365 HCC patients with both expression data and survival data were included in this study. In addition, ESTIMATE algorithm[23] was conducted to calculate the tumor microenvironment scores for each HCC sample using the “estimate” package of R 4.0.5 software (http:///www.r-project.org/).

Analysis of the Relationship Between Tumor Microenvironment Scores and Prognosis of HCC Patients

Tumor microenvironment scores includes stromal scores, immune scores, and Estimate scores. The patients with HCC were divided into high- and low- stromal/immune/ Estimates scores groups based on the best statistical cut-off values, which were calculated by maximally selected rank statistics. The relationship between the stromal/immune/Estimate scores and Overall Survival (OS), Progression-Free Survival (PFS), and Disease- Free Survival (DFS) was validated by Kaplan-Meier survival curves and log-

rank test, P value < 0 .05 was considered statistically significant. In addition, we also assessed the association of the stromal/immune/Estimate scores in HCC samples with their clinicopathologic parameters, such as gender, age, tumor grade, and clinical stages. The results were analyzed and visualized by “limma” and “ggpubr” packages of R 4.0.5 software, and P-value less than 0.05 represents a significant value.

Screening of Differentially Expressed LncRNAs (DElncRNAs) Based on Immune/Stromal Scores

Firstly, the 374 HCC samples from TCGA cohort were divided to high or low immune/stromal scores group according to median scores. Then we performed lncRNAs differential expression analysis of the high scores group and low scores group with the “limma” R package. Wilcox test was applied to obtain p-value, the significant differentially expression lncRNA (DElncRNAs) was defined as Fold Change > | ±1| and a false discovery rate (FDR) < 0.05. The results were visually evaluated with volcano plots and heatmaps by using the “ggplot2” and “pheatmap” R package, the heatmaps displayed the top 20 lncRNAs with positive or negative correlation with high stromal/immune scores according to Fold Change. Subsequently, a Venn diagram was employed to intersect DElncRNA that were upregulated or downregulated in both high immune and stromal score groups, and defined as TME-related DElncRNAs for further analysis.

Establishment and Verification of TME-related DElncRNA prognostic risk model for HCC

To illustrate the prognostic value of DElncRNAs in HCC patients, univariate Cox regression analysis was applied to identify survival-related DElncRNAs. Multivariate Cox regression was adopted to analyzed the contribution of each DElncRNA to prognosis based on the statistics of negative log-likelihood and Akaike Information Criterion (AIC). Finally, we screened out six TME-related DElncRNAs for construct the prognostic risk model. Wilcox test was used to compare differences in lncRNAs expression between normal and tumor tissues. According to the multivariate cox regression coefficient and expression value of each prognostic TME-related lncRNAs, the risk score of each HCC patient was calculated, the equation of risk score was listed as follows:

Risk score = $\sum_{i=0}^{n} \exp \times \beta_i$ (exp is the expressive value of each TME-related DElncRNA, β is the regression coefficient of the lncRNA)

Afterward, HCC patients were divided into high and low-risk groups in line with the median risk score. Then we performed Kaplan-Meier survival analysis to exhibit the association between risk score and overall survival, and $P < 0.05$ was considered statistically different. Receiver Operating Characteristic (ROC) curve was drawn to display the predictive accuracy of the prognostic model via “survivalROC” R package. Meanwhile, stratified analysis was used to estimate the prognostic value of the risk score model for different subgroups based on the following clinicopathological factors: age (< = 65 and > 65), gender

(male and female), grade (grade 1–2 and grade 3–4), clinical stage (stage I-II and stage III-IV), $p < 0.05$ was considered as statistically significant.

Then, Cox's proportional hazards regression model was used to determine the independent prognostic factors for OS in HCC patients, integrating with following clinicopathological factors: age, gender, grade, clinical stage, and risk score group, *P* value < 0 .05 was considered statistically significant.

Nomogram Building and validation

Basing on the risk score and conventional prognostic clinical features (i.e. tumor grade, clinical stage), we established an quantitative scoring system for survival estimation HCC patients via "survival" and "rms" R packages. Then we performed internal verification methods to assess the predictive precision of the nomogram. The Calibration curves and Receiver Operating Characteristic (ROC) curves were drawn to assess the predictive uniformity and accuracy of the nomogram model.

Functional Enrichment analysis

We applied "c2.cp.kegg.v7.4.symbols.gmt " obtained from MsigDB(http://www.gsea-msigdb.org/gsea/msigdb/collections.jsp) of GSEA 4.1.0 software to evaluate functional enrichment pathways of risk score model, $p < 0.05$ indicated statistical significance. Furthermore, the significant differential expression genes (DEGs) were extracted from TCGA sequencing data depending on risk grouping and statistically significant was defined as FDR < 0.05 and $|\log2FC| \geq 1$. According to the DEGs, we conducted Gene Ontology (GO) analysis to evaluate the related biological pathways in two risk groups.

Exploring the Correlation of Risk Score with Tumor Immune Microenvironment

To quantitatively analyze the difference of tumor immune microenvironment status between high- and low-risk group in HCC patients, A range of analytical approaches were undertaken. Firstly, single-sample gene set enrichment analysis (ssGSEA) was conducted to explore the difference in infiltrating level of immune cells and immune-related pathways between the two risk groups by using "gsva" and "GSEABase" R package[24], and the result was visualized with boxplot by "ggpubr" R package. Then, we obtained the Immune cell infiltration information of each tumor sample from Tumor Immune Estimation Resource (TIMER) (https://cistrome.shinyapps.io/timer/), CIBERSORT (https://cibersort.stanford.edu/) was performed to identify and calculate the relative proportions of 22 tumor-infiltrating immune cells (TIICs) in each HCC patient, Spearman analysis was performed to elucidate the correlation of proportions of TIICs with risk score. Furthermore, to evaluate the potential role of the prognosis signature in immune checkpoint blockade therapy of HCC, differential expression analysis of immune checkpoint blockade–related genes was implied in high-risk samples and low-risk samples. Moreover, immunophenoscore (IPS), including IPS-CTLA4(-)/PD1(-), IPS-CTLA4(-)/PD1(+),IPS-CTLA4(+)/PD1(-), IPS-CTLA4(+)/PD1(+), was calculated to predict the treatment response of immune checkpoint inhibitors (ICIs) in HCC patients, which downloaded from the Cancer Immunome Atlas database (TCIA, https://tcia.at/home). T-test was

adopted to compare the IPS scores of the two risk groups, *P* value < 0 .05 was considered statistically significant in all above analysis.

Statistical Analysis

The statistical analyses were performed using R software (https://www.r-project.org/, version 4.0.4), SPSS version 23. Chi-square test was used to analyze the baseline characteristics of HCC patients. Student's t-test or rank-sum test was applied to compare difference between the two groups. Cox regression analyses were performed to build a prognostic model. Kaplan-Meier analysis were employed to evaluate the survival difference between two risk groups. ROC curve was used to estimate the risk models' predictive abilities. All statistical tests were two-sided and statistical significance was set at $p < 0.05$.

Results

Stromal/Immune/Estimate Scores of Tumor Microenvironment Were Significantly Correlated with Prognosis in HCC Patients

Transcriptome data and corresponding clinical information of HCC were downloaded from the TCGA database and UCSC Xena database, respectively. After removing repeated samples and patients with less than 0 day follow-up time, a total of 365 patients with complete transcriptome and clinical data were incorporated into subsequent survival analysis. According to ESTIMATE algorithm, stromal/ immune/Estimate scores were calculated (**Additional File 1: Table S1**). 365 HCC patients were divided into high- and low-score groups based on the best statistical cut-off values, which was − 914.61(ranged from − 1622.33 to 1180.26) in stromal groups, 41.48(ranged from − 861.77 to 3157.28) in immune groups, and

-909.71(ranged from − 2165.59 to 3722.93) in Estimate groups. Subsequently, Kaplan-Meier survival curves analyzed the association of Stromal/Immune/Estimate scores with OS (Fig. 2A-C), PFS (Fig. 2D-F), and DFS (Fig. 2G-I), the results showed the high Stromal/Immune/ Estimate scores were significantly associated with better prognosis of the HCC patients (Fig. 2). Next, we investigated whether there was any association between Stromal/Immune/Estimate scores with the clinicopathological characteristics of HCC patients. As shown in Fig. 3A-L, there was no significant correlation between Estimate score with gender (male vs female), age (> = 65 vs < 65), tumor grade (Grade 1–2 vs. Grade 3–4), clinical stages (Stage I-II vs. Stage III-IV). Moreover, no difference was observed of immunes scores and stromal scores in age and gender subgroup. But we noticed that patients in high-stage (Stage III-IV) had lower immune scores compared with Stage I-II ($p = 0.031$), and higher grade (grade 3–4) was associated with lower stromal scores than the low grade (Grade 1–2) in patients with HCC ($p = 0.013$).

DELncRNAs were Identification Based on High and Low Immune/Stromal Scores

Totally, 3848 lncRNAs were acquired from the TCGA transcriptome dataset after data processing. Firstly, we grouped the 374 HCC samples into high scores or low scores group according to the median values of stromal scores and immune scores, and then differentially expressed lncRNAs were filtered out between two group with Fold Change > | ±1|. The results were visualized with volcano plot and Heatmap, a total of 101 downregulated and 123 upregulated lncRNAs were identified in the stromal scores group (Fig. 4A, **Additional File 2: Table S2**), and 47 downregulated and 122 upregulated lncRNAs in high immune score groups compared to low scores group (Fig. 4B, **Additional File 3: Table S3**). Among them, the intersecting lncRNAs were considered as most likely associated with tumor microenvironment of HCC. Thus, compared with low scores group, there were a total of 24 commonly downregulated lncRNAs and 76 commonly upregulated lncRNA both in the high immune and stromal scores groups, which were selected as TME-related differential expression LncRNAs (DElncRNAs), as displayed in the Venn diagrams (Fig. 4C-D, **Additional File 4: Table S4**).

Construction a Prognostic Risk Signature Using the DElncRNAs and Exploring Its Prognostic Value.

In order to further investigated the association between DElncRNAs with prognosis in HCC patients, univariate and multivariate analysis were performed to established prognostic signature. Firstly, Among the 100 TME-related lncRNAs, 9 lncRNAs were identified as prognostic-associated candidates by univariate Cox regression analysis with $p < 0.05$, the result was displayed in Table 1. Subsequently, six lncRNAs (LINC01150, LINC02273, LINC00426, AP002954.1, AC007277.1, and AC008549.1) were obtained to construct a prognostic signature by using multivariate Cox regression analysis with the minimum AIC value (AIC = 1254). Among them, LINC02273, LINC00426, and AC008549.1 were prognostic lncRNAs with hazard ratio (HR) < 1, whereas LINC01150, AP002954.1, and AC007277.1 were poor prognostic factors with HR > 1(Table 2).

Table 1
Univariate Cox regression analysis of TME-related lncRNAs.

LncRNA	HR	HR.95L	HR.95H	*P* value
LINC01150	2.279	1.421	3.655	0.0006
LINC02273	0.245	0.062	0.973	0.046
LINC00426	0.187	0.037	0.938	0.042
LINC01094	2.007	1.393	2.891	0.0002
LINC00892	0.246	0.061	0.989	0.048
LINC01871	0.907	0.823	0.999	0.049
AP002954.1	1.583	1.000	2.504	0.05
AC007277.1	1.242	1.009	1.527	0.04
AC008549.1	0.985	0.972	0.998	0.025

LncRNA: Long noncoding RNAs; HR: hazard ratio; HR.95L: low 95% CI of HR; HR.95H: high 95% CI of HR.

Table 2
Multivariate Cox regression analysis of TME-related lncRNAs.

LncRNA	Coefficient	HR	HR.95L	HR.95H	P value
LINC01150	0.947	2.579	1.524	4.365	0.0004
LINC02273	-1.838	0.159	0.024	1.036	0.054
LINC00426	-3.083	0.046	0.005	0.451	0.008
AP002954.1	1.255	3.507	1.71	7.192	0.0006
AC007277.1	0.179	1.195	0.997	1.433	0.054
AC008549.1	-0.014	0.986	0.974	0.999	0.039

LncRNA: Long noncoding RNAs; HR: hazard ratio; HR.95L: low 95% CI of HR; HR.95H: high 95% CI of HR.

According to six TME-related lncRNAs and multivariate Cox regression coefficient, the individualized risk score was calculated as follows: risk score = (0.947 × LINC01150 expression) + (-0.838 × LINC02273 expression) + (-3.083 × LINC00426 expression) + (1.255 × AP002954.1 expression) + (0.178 ×AC007277.1 expression) + (-0.014× AC008549.1 expression). Then we calculated the risk score of each patient and the 365 HCC patients were divided into two groups according to the median score, 183 in low-risk group and 182 in high-risk group (the median value = 1.119). Kaplan-Meier survival curves for overall

survival (OS) suggested that HCC patients in high-risk group had worse prognosis than those with low-risk(p = 5.506E − 06) as shown in Fig. 5A. ROC curve analysis demonstrated that the prognostic model were expected to provide accurate predictions with AUC = 0.707 (Fig. 5B). And risk score curves and scatter plots revealed that the higher risk score, the more death was occurred in HCC patients (Fig. 5C-D). The heatmap demonstrated that the expression of LINC01150, AP002954.1, and AC007277.1 was up-regulated in high-risk group, while the other three lncRNAs (LINC02273, LINC00426, and AC008549) were up-regulated in low-risk group (Fig. 5E). Furthermore, univariate and multivariate Cox proportional hazards regression analyses were carried out to explore the independent prognostic factors for the overall survival of HCC patients. The results showed the risk signature and clinical stage were independent predictors (Fig. 5F-G). The above results manifested the TME-related lncRNAs risk model had an accurate predictive ability for HCC patient' s prognosis.

Furthermore, we categorized patients into different subgroups on the basis of age (< = 65 and > 65), gender (male and female), grade (Grade 1–2 and Grade 3–4), clinical stage (Stage I-II and Stage III-IV), and tumor stage (T1-2, T3-4), then Kaplan-Meier survival curves was conducted in different subgroup to further investigate the prognostic value of the risk model. As shown in Fig. 6A-H, patients with different age, tumor stage, and clinical stage in the high-risk group had worse survival than those in the low-risk group, and similar results were obtained in the Male group and Grade1-2. Whereas there was no significant difference in female patients and patients with Grade 3–4. Besides, the association between risk signature and clinical features was assessed, we noticed that prognostic model was significantly related with gender(P = 0.048), tumor stage (P < 0.001) and clinical stage (P = 0.011), whereas the risk model was not correlated with age or tumor grade (Fig. 6I-N). Collectively, it can be concluded that the risk signature was suitable for diverse populations of HCC, and those lncRNAs in the risk model may play a crucial role in HCC progression.

The Prognostic Nomogram Accurately Predict HCC patients Outcomes.

We quantitatively calculated the 1-,2- and 3-year survival probability of HCC patients according to grade, clinical stage, and risk score by establishing a nomogram. The comprehensive score was figured up basing on each score of clinical factors. The nomogram showed the higher of the total points, the worse of the prognosis (Fig. 7A). The consistency and accuracy of nomogram was assessed by calibration curve and Receiver Operating Characteristic (ROC) curves. The calibration curves displayed the predictive ability of the nomogram model nearly in accordance with reality (Fig. 7B-D), and Receiver Operating Characteristic (ROC) curves analysis indicated the nomogram achieved better prediction performance with AUC = 0.720 for 1-years OS, AUC = 0.712 for 2-years OS, and 0.740 for 3-years OS, as shown in Fig. 7E-G. Overall, the nomogram exhibited preferable clinical practicality in predicting the prognosis of HCC.

Potential Biological Pathway and Functional Enrichment Analysis Based on Risk Signature

Firstly, GSEA analysis was conducted to probe the potential biological mechanism of the TME-related lncRNAs signature, the results revealed that tumor-related pathways, including bladder cancer, renal cell carcinoma, cell cycle, DNA replication, ERBB and Notch signaling pathway, were highly enriched in the high-risk group with $p < 0.05$, as shown in Fig. 8A. To further determine the biofunctions associated with the risk signature, differentially expressed genes were selected based on criteria of $P < 0.05$ and fold change > 1 between the low- and high-risk group from TCGA database. A total of 256 DEGs (upregulated 119 genes, downregulated 136 genes) were identified in the high-risk group compared with low-risk group. Then, we selected the DEGs for GO enrichment analysis. The results indicated that some immune-related pathways were enriched, such as “humoral immune response”, “complement activation”, “adaptive immune response”, and “B cell mediated immunity” (Fig. 8B). Thus, we could conclude that the prognostic TME-related lncRNAs signature may play important roles not only in the reshaping and changing the tumor immune microenvironment but also in tumorigenesis and progression of HCC.

The Prognostic Risk Signature Affecting Tumor Immune Features

To probe into the correlation of risk scores and tumor immune microenvironment status, we evaluated the difference of immune cells between high- and low-risk group in HCC patients with Single-sample gene set enrichment analysis (ssGSEA) and CIBERSORT algorithm. From the ssGSEA results, we found the infiltration level of immune cells, including B cells, CD8 + T cells, mast cells, Follicular helper T cells (Tfh), Th1 cells, and tumor infiltrating lymphocyte (TIL) were remarkably upregulated in low-risk group, and the immune-related pathways (i.e. immune checkpoint pathway, Cytolytic activity, inflammation-promoting, T cell co-inhibition/stimulation, INF-II response) were significantly activated in low-risk group compared with high-risk group ($P < 0.05$) (Fig. 9A). The CIBERSORT analysis results suggested that the following immune cells infiltration levels: naive B cells (R= -0.16; P = 0.0021), activated memory CD4 + T cells (R= -0.2; P = 1e-04), CD8 + T cells (R= -0.23; P = 7.1e-06),

γδ T cells(R= -0.16; P = 0.003), were negatively relevant to risk score, whereas significant positive correlations were observed between the proportions of memory B cells (R = 0.16; P = 0.0021), M0 Macrophages (R = 0.26; P = 7.3e-07), M2 Macrophages (R = 0.17; P = 0.0011) and risk score (Table 3, Fig. 9B-H).

Table 3
Correlation analysis of 22 immune cells infiltration levels with risk scores

Immune Cell	*R*	*P* Value
B cells naive	-0.16	0.002095003
B cells memory	0.16	0.002336936
Plasma cells	-0.1	0.05199941
T cells CD8	-0.23	7.15E-06
T cells CD4 naive	-0.059	0.263867315
T cells CD4 memory resting	0.013	0.810632983
T cells CD4 memory activated	-0.2	0.000102883
T cells follicular helper	-0.013	0.807812793
T cells regulatory (Tregs)	-0.055	0.30002029
T cells gamma delta	-0.16	0.002975049
NK cells resting	-0.088	0.095016394
NK cells activated	0.0096	0.855642376
Monocytes	0.061	0.250214059
Macrophages M0	0.17	0.001087181
Macrophages M1	-0.065	0.216904497
Macrophages M2	0.26	7.33E-07
Dendritic cells resting	-0.017	0.743538196
Dendritic cells activated	0.1	0.051715294
Mast cells resting	-0.023	0.666050316
Mast cells activated	0.00092	0.986067845
Eosinophils	-0.037	0.4874298
Neutrophils	0.089	0.09158816
R: Spearman's rank correlation Rho;		

Given the difference of immune check-point pathway between high- and low-risk group, we further compared the expression levels of 46 immune

checkpoint blockade–related genes in two groups, and concentrated on the assessment of the four pivotal immune checkpoint inhibitor genes (PD1, PD-L1, PD-L2, and CTLA4). The results demonstrated

that 20 out of the 46 immune checkpoint blockade-related genes were significantly different between two risk groups with P-value < 0.05(Fig. 10A). Among the four key genes, the expression level of PD-L2, and CTLA4 was significantly up-regulated in low-risk group (Fig. 10B-E), which indicated the risk signature might play a vital role in predicting treatment outcome of immune checkpoint blockade in HCC. Thus, we further explored the association of the risk signature and the treatment responses to immune checkpoint inhibitors (ICIs) in HCC by comparing the immunophenoscore (IPS) between the high-risk and low-risk group. The result showed the HCC patients in the low-risk group exhibited higher IPS, involving in four IPS subgtypes (IPS-CTLA4(-)/PD1(+), IPS-CTLA4(-)/PD1(+), IPS-CTLA4(+)/PD1(-), IPS-CTLA4(+)/PD1(+)), which manifested that HCC patients in the low-risk group are more likely to benefit from ICIs (Fig. 10F-I).

Discussion

Immune microenvironment plays an important role in the tumor progression, immune escape and immunotherapy resistance[10]. Hepatocellular carcinoma (HCC) is a typical inflammatory related malignancy, in which contains a large number of macrophages, innate and adaptive immune cells, thus forming a complex immune tolerance microenvironment[25]. In recent years, with the rapid development of bioinformatics on tumor immunity microenvironment, immunotherapy has gained a lot of interest from researchers due to its great potential for effectively treating HCC. Nevertheless, there remain many unanswered questions, such as low objective response rate, high adverse reaction, and high resistance rates, which obstruct the generalization of immunotherapy. Thus, deeper understanding of the role of the tumor microenvironment will improve the response rates of the current treatment approaches, and provide great clinical significance for precise treatment of HCC patients.

In this research, according to gene expression analysis of TCGA database, the ESTIMATE algorithm was applied to calculated the immune/stromal/Estimate scores of TME in HCC. Then, we explored the impact of the immune/stromal/Estimate scores on OS, PFS, and DFS, and further analyzed the correlation of immune/stromal/Estimate with clinicopathologic parameters (i.e. gender, age, tumor grade, and clinical stages). The results indicated the higher score of stromal/immune/Estimate were significantly associated with longer survival, including OS, PFS, and DFS in patients with HCC. Moreover, immune/stromal scores were inversely correlated with tumor grade and clinical stage, which manifested that stromal/immune/Estimate scores might predicate the survival of HCC patients and the malignancy of tumors. Given that lncRNAs could influence tumor microenvironment and finally affect tumor behaviors, we opted to focus on searching DElncRNAs basing on high- or low- stromal and immune scores, which were identified as TME-related lncRNAs, and then exploring the prognosis values of those DElncRNAs. Eventually, we identified six EMT-related lncRNAs (LINC01150, LINC02273, LINC00426, AP002954.1, AC007277.1, and AC008549.1) to construct the prognostic signature via Cox regression analysis. Then the risk scores were calculated based on the expression profiles and coefficients of the six lncRNAs. Kaplan–Meier analysis, ROC curve analysis, univariate and multivariate Cox regression analysis were carried out to explored the prognostic values of the risk signature, the results indicated that the

survival in high-risk group were worse than those of patients in low-risk group, and the risk score model could correctly predict the OS as independent indicator of HCC patients compared with other clinical parameters. In addition, in order to better apply the risk model in clinical practice, we established a nomogram based on risk score and other clinical feathers (i.e. grade and clinical stage) and verified the nomogram with calibration curve and ROC curve, the identification results showed that the nomogram had a satisfactory uniformity with actual survival and provided a better clinical practicality than the traditional tumor grade or clinical stage system.

Some lncRANs in this risk model have been illuminated to be involved in the progression of HCC or other cancers, including LINC00426 and LINC02273. Previous study have demonstrated that the expression of LINC00426 was significantly down-regulated in the tumor tissue of including 72 NSCLC patients compared to normal lung tissue and the expression level was also remarkably correlated with the clinical stage[26].In contrast, another study showed an opposite result, the LINC00426 was significantly up-regulated in lung adenocarcinoma(LUAD) tissues and cell lines and play a notable role in accelerating tumor proliferation, invasion, metastasis, and epithelial–mesenchymal transition (EMT) in vitro and in vivo, which via regulating the miR-455-5p/ UBE2V1[27]. Besides, it has been reported that LINC00426 is also a key regulator in doxorubicin resistance of osteosarcoma [28]. Significantly, LINC00426 might reshape the tumor immune microenvironment, which positively associated with T-helper cell differentiation, cytokine signaling pathways, and multiple immune markers, including cytotoxic markers, coinhibitory and costimulatory molecules (i.e. PDCD1, CTLA4, HAVCR2, TIGIT, FOXP3, ICOS), and chemokine receptors and ligands (i.e. CXCR3/6, CXCL9/13, CCL4/5/7/19, CCR7)[29]. Another study revealed that LINC00426 significantly correlated with immune cell fraction in clear cell renal cell carcinoma based on bioinformatic analysis[30]. In this study, we found LINC 00426 was significantly upregulated in both high immune scores groups and high stromal scores group compared to low scores groups, which might play a key role in altering tumor microenvironment, this result were consistent with those previously reported. Another prognostic lncRNA LINC002273 was reported correlation with tumor proliferation, migration, and invasion by epigenetically increasing AGR2 transcription in breast cancer[31]. Nevertheless, the other four prognostic TME-related lncRNAs (LINC01150, AP002954.1, AC007277.1, and AC008549.1) were rarely reported. Thus, our research may provide a new perspective for their potential functions.

Subsequently, GSEA analysis was conducted to deeply probe the underlying mechanism and functional enrichment of the risk signature built by the six lncRNAs in HCC. The results indicated that some pathways associated with HCC tumorigenesis and progression might be activated in high-risk group, including ERBB signaling pathway, Notch signaling pathway, DNA replication and cell cycle. Besides, the GO analysis suggested that DEGs, which screened out between high- and low-risk group, were mainly involved in immune features, such as “humoral immune response”, “complement activation”, “adaptive immune response”, and “B cell mediated immunity”. Tumor cells interact with TME through various paracrine signaling pathways, among which Notch signaling pathway is considered to be one of the important pathways. The role of Notch signaling pathway in promoting or inhibiting cancer in tumor cells has been widely recognized[32]. Moreover, previous studies also have demonstrated that Notch signal is

involved in regulating the differentiation and function of lymphocytes, DCs, Th cells and Treg cells[33–36]. Notch signaling is vital for the regulating activation of cytotoxic T cell (CTL), that Dll1 binging to Notch1 or Notch2 to express granzyme B and IFN- γ is necessities for naive CD8 + cells activation and differentiation, thereby enhancing antigen-specific cytotoxicity and inhibiting tumor growth[35, 37]. Nevertheless, a study in colon cancer found even if inhibits the Notch signal of CD8 + T cells, T cells can enhance their cytotoxic activity by reducing the expression of PD-1[38]. Therefore, the function of Notch signaling pathway in a specific tumor microenvironment needs to be further clarified.

Given the significant role of the tumor microenvironment in the process of tumorigenesis, we constructed TME-related lncRNAs risk signature. We then analyzed the correlation between the risk signature and specific immune cells or immune pathways with ssGSEA and CIBERSORT algorithm. We discovered that some immune cells, which were beneficial to enhance immune responses towards cancer, were remarkably upregulated in low-risk group, including B cells, CD8 + T cells, mast cells, Follicular helper T cells (Tfh), Th1 cells, and tumor infiltrating lymphocyte (TIL). CIBERSORT analysis indicated certain immune cells infiltration levels were negatively relevant to risk score, such naive B cells, activated memory CD4 + T cells, CD8 + T cells, γδ T cells, which can be understood as the higher the risk score, the lower infiltration level of immune response cells. Conversely, M2 macrophages were significant positive correlated with risk score, which contribute to tumor angiogenesis, metastasis, epithelial-mesenchymal transition (EMT), and immune suppression in HCC[39]. The differences of immune cells in tumor microenvironment between high-risk and low-risk group may partly account for why HCC patients in high-risk group showed worse prognosis than those low-risk group patients. In addition, we found the immune-related pathways (i.e. immune checkpoint pathway, Cytolytic activity, inflammation-promoting, T cell co-inhibition/stimulation, INF-II response) were significantly activated in low-risk group compared with high-risk group. Among them, immune checkpoint pathway is one of the hotspots in recent years, immune checkpoint inhibitors (ICIs) can restore the immune recognition and attack ability of T cells through blocking the inhibition of checkpoint, so as to enhance the anti-tumor ability. Nevertheless, only a minority of HCC patients can benefit from the immune therapy and less than 30% of patients were observed for objective response to immune checkpoint inhibitors treatment. Thus, exploring more accurate biomarkers to forecast responsiveness of ICBs treatment and further screen the dominant population has become a major challenge in the treatment of HCC. In this study, we found 20 out of the 46 immune checkpoint blockade-related genes were significantly different between high- and low-risk group, and the expression level of PD-L2, and CTLA4 was significantly up-regulated in low-risk group. Furthermore, immunophenoscore (IPS) was compared to explore the correlation between risk score and ICIs immunotherapy response in HCC. Our results showed the HCC patients in the low-risk group exhibited higher IPS and tended to have better response after ICIs treatment. These findings manifested that the prognostic TME-related lncRNAs may possess the ability to predict clinical outcome of ICIs therapy in HCC samples.

In conclusion, we conducted overall analysis the impact of immune and stromal scores of the tumor microenvironment on the prognosis of patients with HCC. 100 DElncRNAs were filtered according to different expression both in high immune and stomal score group compared with low score groups, and

eventually six lncRNAs was used to establish a novel TME-related prognostic risk signature basing on Cox regression analysis, which may improve prognostic predictive accuracy and guide individualized immunotherapy for HCC patients.

Abbreviations

HCC: Hepatocellular carcinoma;

TME: tumor microenvironment;

LncRNAs: Long noncoding RNAs;

TCGA: The Cancer Genome Atlas;

OS: Overall Survival (OS);

PFS: Progression Free Survival;

DFS: Disease Free Survival;

DElncRNAs: Differentially Expressed LncRNAs;

HR: hazard ratio;

ROC: Receiver Operating Characteristic;

AUC: area under the curve;

GSEA: Gene set enrichment analysis;

GO: Gene Ontology;

DEGs: Differential expression genes;

ssGSEA: Single-sample gene set enrichment analysis;

ICIs: Immune checkpoint inhibitors;

IPS: Immunophenoscore;

Declarations

Competing interests

The authors declare no competing interests.

Funding

This research was supported by the National Natural Science Foundation of China (NO. 82060435)

Authors' contributions

JB W conceived and designed the study. SL H and J Z were responsible for the collection and analysis of the research information. SL H involved in drafting the manuscript. D L, XL L, LL Z, and JB W critically and carefully revised this manuscript. The authors read and approved the final manuscript.

Acknowledgements

We acknowledge and appreciate our colleagues for their valuable efforts and comments on this paper.

Ethical approval statement

The study was approved by the ethics committee of the Second Affiliated Hospital of Nanchang University.

Availability of data and materials

The datasets presented in this study can be found in online repositories. The names of the repository/repositories and accession number(s) can be found in the article/Supplementary Material.

References

1. Yoon JS, Sinn DH, Lee JH, Kim HY, Lee CH, Kim SW, et al. Tumor Marker-Based Definition of the Transarterial Chemoembolization-Refractoriness in Intermediate-Stage Hepatocellular Carcinoma: A Multi-Cohort Study. Cancers (Basel). 2019;11(11).
2. Siegel RL, Miller KD, Jemal A. Cancer statistics, 2018. CA Cancer J Clin. 2018;68(1):7-30.
3. Bray F, Ferlay J, Soerjomataram I, Siegel RL, Torre LA, Jemal A. Global cancer statistics 2018: GLOBOCAN estimates of incidence and mortality worldwide for 36 cancers in 185 countries. CA Cancer J Clin. 2018;68(6):394-424.
4. Villanueva A, Longo DL. Hepatocellular Carcinoma. New England Journal of Medicine. 2019;380(15):1450-62.
5. Jemal A, Ward EM, Johnson CJ, Cronin KA, Ma J, Ryerson B, et al. Annual Report to the Nation on the Status of Cancer, 1975-2014, Featuring Survival. J Natl Cancer Inst. 2017;109(9).
6. Qin S, Xu L, Yi M, Yu S, Wu K, Luo S. Novel immune checkpoint targets: moving beyond PD-1 and CTLA-4. Mol Cancer. 2019;18(1):155.
7. El-Khoueiry AB, Sangro B, Yau T, Crocenzi TS, Kudo M, Hsu C, et al. Nivolumab in patients with advanced hepatocellular carcinoma (CheckMate 040): an open-label, non-comparative, phase 1/2 dose escalation and expansion trial. Lancet. 2017;389(10088):2492-502.

8. Zhu AX, Finn RS, Edeline J, Cattan S, Ogasawara S, Palmer D, et al. Pembrolizumab in patients with advanced hepatocellular carcinoma previously treated with sorafenib (KEYNOTE-224): a non-randomised, open-label phase 2 trial. Lancet Oncol. 2018;19(7):940-52.
9. Khemlina G, Ikeda S, Kurzrock R. The biology of Hepatocellular carcinoma: implications for genomic and immune therapies. Mol Cancer. 2017;16(1):149.
10. Kurebayashi Y, Ojima H, Tsujikawa H, Kubota N, Maehara J, Abe Y, et al. Landscape of immune microenvironment in hepatocellular carcinoma and its additional impact on histological and molecular classification. Hepatology. 2018;68(3):1025-41.
11. Galdiero MR, Bonavita E, Barajon I, Garlanda C, Mantovani A, Jaillon S. Tumor associated macrophages and neutrophils in cancer. Immunobiology. 2013;218(11):1402-10.
12. Ovais M, Guo M, Chen C. Tailoring Nanomaterials for Targeting Tumor-Associated Macrophages. Adv Mater. 2019;31(19):e1808303.
13. Lee WC, Wu TJ, Chou HS, Yu MC, Hsu PY, Hsu HY, et al. The impact of CD4+ CD25+ T cells in the tumor microenvironment of hepatocellular carcinoma. Surgery. 2012;151(2):213-22.
14. Yuan L, Xu ZY, Ruan SM, Mo S, Qin JJ, Cheng XD. Long non-coding RNAs towards precision medicine in gastric cancer: early diagnosis, treatment, and drug resistance. Mol Cancer. 2020;19(1):96.
15. Necula L, Matei L, Dragu D, Neagu AI, Mambet C, Nedeianu S, et al. Recent advances in gastric cancer early diagnosis. World J Gastroenterol. 2019;25(17):2029-44.
16. Fan Y, Wang YF, Su HF, Fang N, Zou C, Li WF, et al. Decreased expression of the long noncoding RNA LINC00261 indicate poor prognosis in gastric cancer and suppress gastric cancer metastasis by affecting the epithelial-mesenchymal transition. J Hematol Oncol. 2016;9(1):57.
17. Wu M, Fu P, Qu L, Liu J, Lin A. Long Noncoding RNAs, New Critical Regulators in Cancer Immunity. Front Oncol. 2020;10:550987.
18. Wang Y, Yang L, Dong X, Yang X, Zhang X, Liu Z, et al. Overexpression of NNT-AS1 Activates TGF-β Signaling to Decrease Tumor CD4 Lymphocyte Infiltration in Hepatocellular Carcinoma. Biomed Res Int. 2020;2020:8216541.
19. Lippitz BE. Cytokine patterns in patients with cancer: a systematic review. Lancet Oncol. 2013;14(6):e218-28.
20. Carpenter S, Aiello D, Atianand MK, Ricci EP, Gandhi P, Hall LL, et al. A long noncoding RNA mediates both activation and repression of immune response genes. Science. 2013;341(6147):789-92.
21. Tang Y, He Y, Shi L, Yang L, Wang J, Lian Y, et al. Co-expression of AFAP1-AS1 and PD-1 predicts poor prognosis in nasopharyngeal carcinoma. Oncotarget. 2017;8(24):39001-11.
22. Wang CJ, Zhu CC, Xu J, Wang M, Zhao WY, Liu Q, et al. The lncRNA UCA1 promotes proliferation, migration, immune escape and inhibits apoptosis in gastric cancer by sponging anti-tumor miRNAs. Mol Cancer. 2019;18(1):115.
23. Yoshihara K, Shahmoradgoli M, Martínez E, Vegesna R, Kim H, Torres-Garcia W, et al. Inferring tumour purity and stromal and immune cell admixture from expression data. Nat Commun. 2013;4:2612.

24. Rooney MS, Shukla SA, Wu CJ, Getz G, Hacohen N. Molecular and genetic properties of tumors associated with local immune cytolytic activity. Cell. 2015;160(1-2):48-61.
25. Nishida N, Kudo M. Immunological Microenvironment of Hepatocellular Carcinoma and Its Clinical Implication. Oncology. 2017;92 Suppl 1:40-9.
26. Du W, Sun J, Gu J, Zhang S, Zhang T. Bioinformatics analysis of LINC00426 expression in lung cancer and its correlation with patients' prognosis. Thorac Cancer. 2020;11(1):150-5.
27. Li H, Mu Q, Zhang G, Shen Z, Zhang Y, Bai J, et al. Linc00426 accelerates lung adenocarcinoma progression by regulating miR-455-5p as a molecular sponge. Cell Death Dis. 2020;11(12):1051.
28. Wang L, Luo Y, Zheng Y, Zheng L, Lin W, Chen Z, et al. Long non-coding RNA LINC00426 contributes to doxorubicin resistance by sponging miR-4319 in osteosarcoma. Biol Direct. 2020;15(1):11.
29. Wang B, Mou H, Liu M, Ran Z, Li X, Li J, et al. Multiomics characteristics of neurogenesis-related gene are dysregulated in tumor immune microenvironment. NPJ Genom Med. 2021;6(1):37.
30. Xiang Z, Shen E, Li M, Hu D, Zhang Z, Yu S. Potential prognostic biomarkers related to immunity in clear cell renal cell carcinoma using bioinformatic strategy. Bioengineered. 2021;12(1):1773-90.
31. Xiu B, Chi Y, Liu L, Chi W, Zhang Q, Chen J, et al. LINC02273 drives breast cancer metastasis by epigenetically increasing AGR2 transcription. Mol Cancer. 2019;18(1):187.
32. Ntziachristos P, Lim JS, Sage J, Aifantis I. From fly wings to targeted cancer therapies: a centennial for notch signaling. Cancer Cell. 2014;25(3):318-34.
33. Tchekneva EE, Goruganthu MUL, Uzhachenko RV, Thomas PL, Antonucci A, Chekneva I, et al. Determinant roles of dendritic cell-expressed Notch Delta-like and Jagged ligands on anti-tumor T cell immunity. J Immunother Cancer. 2019;7(1):95.
34. Wang YC, He F, Feng F, Liu XW, Dong GY, Qin HY, et al. Notch signaling determines the M1 versus M2 polarization of macrophages in antitumor immune responses. Cancer Res. 2010;70(12):4840-9.
35. Cho OH, Shin HM, Miele L, Golde TE, Fauq A, Minter LM, et al. Notch regulates cytolytic effector function in CD8+ T cells. J Immunol. 2009;182(6):3380-9.
36. Sierra RA, Trillo-Tinoco J, Mohamed E, Yu L, Achyut BR, Arbab A, et al. Anti-Jagged Immunotherapy Inhibits MDSCs and Overcomes Tumor-Induced Tolerance. Cancer Res. 2017;77(20):5628-38.
37. Biktasova AK, Dudimah DF, Uzhachenko RV, Park K, Akhter A, Arasada RR, et al. Multivalent Forms of the Notch Ligand DLL-1 Enhance Antitumor T-cell Immunity in Lung Cancer and Improve Efficacy of EGFR-Targeted Therapy. Cancer Res. 2015;75(22):4728-41.
38. Yu W, Wang Y, Guo P. Notch signaling pathway dampens tumor-infiltrating CD8(+) T cells activity in patients with colorectal carcinoma. Biomed Pharmacother. 2018;97:535-42.
39. Li Z, Wu T, Zheng B, Chen L. Individualized precision treatment: Targeting TAM in HCC. Cancer Lett. 2019;458:86-91.

Figures

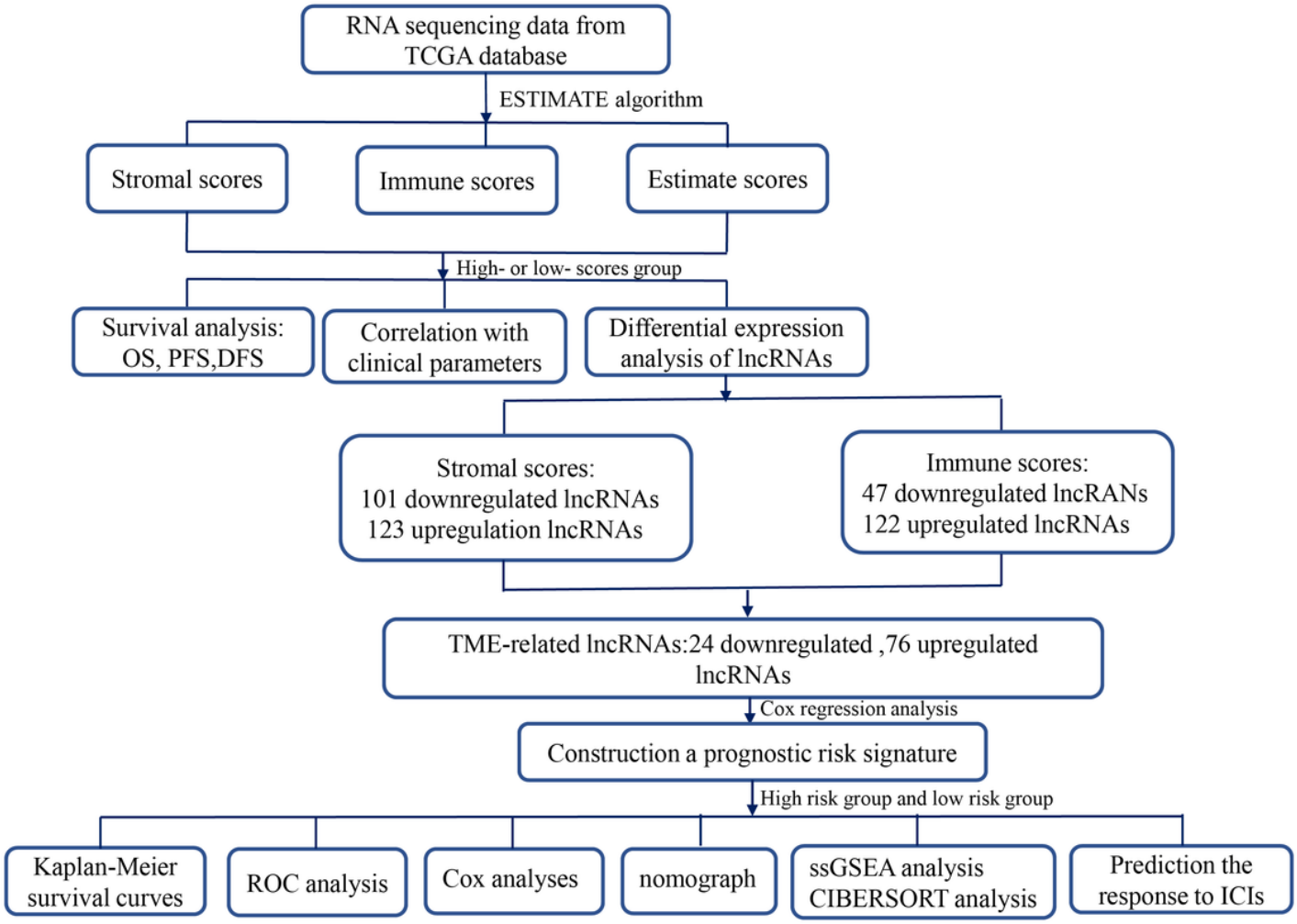

Figure 1

Flowchart of this analysis. TME: tumor microenvironment; LncRNAs: long noncoding RNAs; TCGA: The Cancer Genome Atlas; OS: Overall Survival (OS); PFS: Progression Free Survival; DFS: Disease Free Survival; ROC: Receiver Operating Characteristic; COX: univariate and multivariate Cox proportional hazards regression; GSEA: Gene set enrichment analysis; GO: Gene Ontology; ICIs: Immune checkpoint inhibitors.

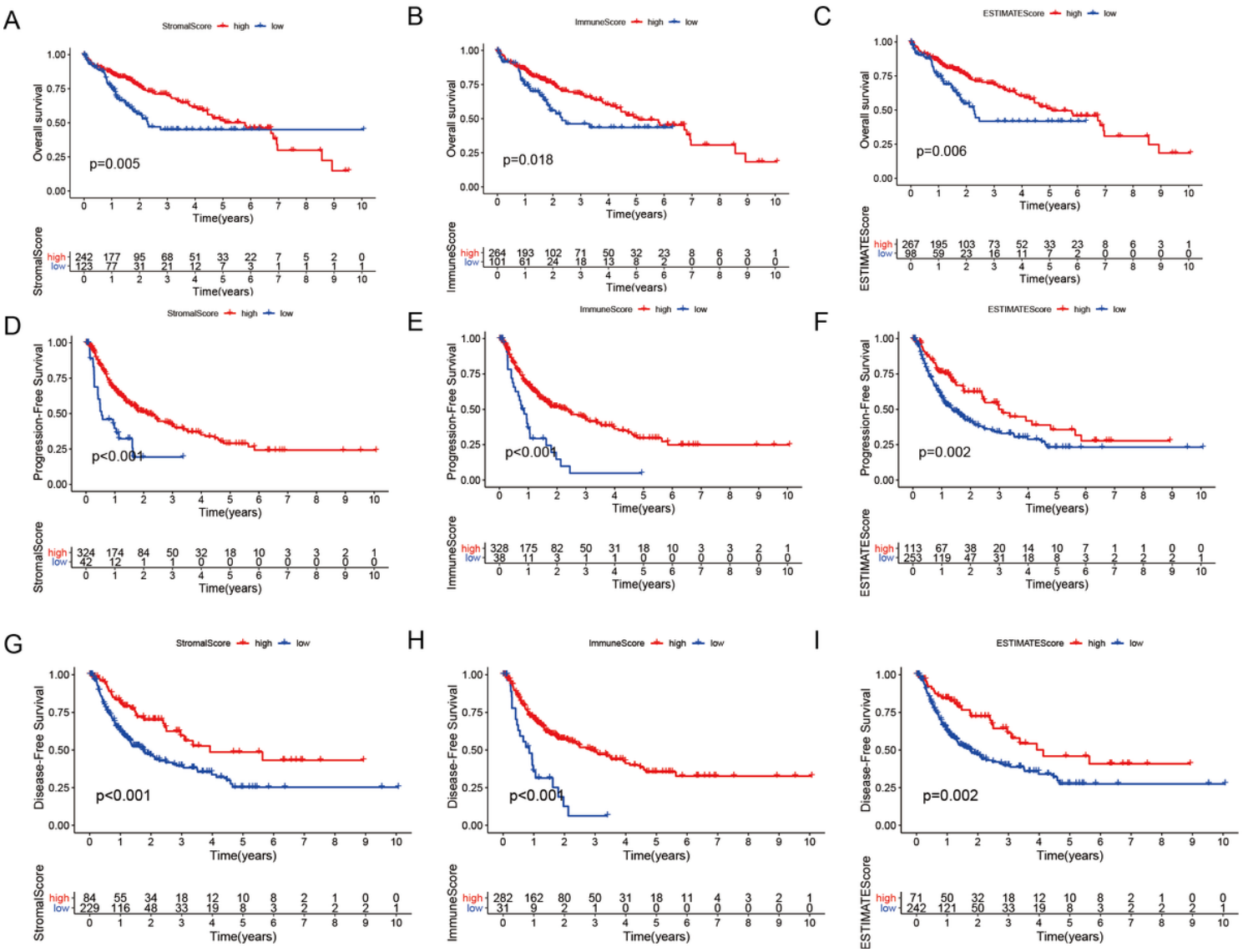

Figure 2

Kaplan-Meier survival curves analysis of stromal/immune/Estimate scores with HCC patient prognosis. (A-C) The correlation of stromal/immune/Estimate scores with Overall Survival. (D-F) The correlation of stromal/immune/Estimate scores with Progression Free Survival. (G-I) The correlation of stromal/immune/Estimate scores with Disease Free Survival (DFS).

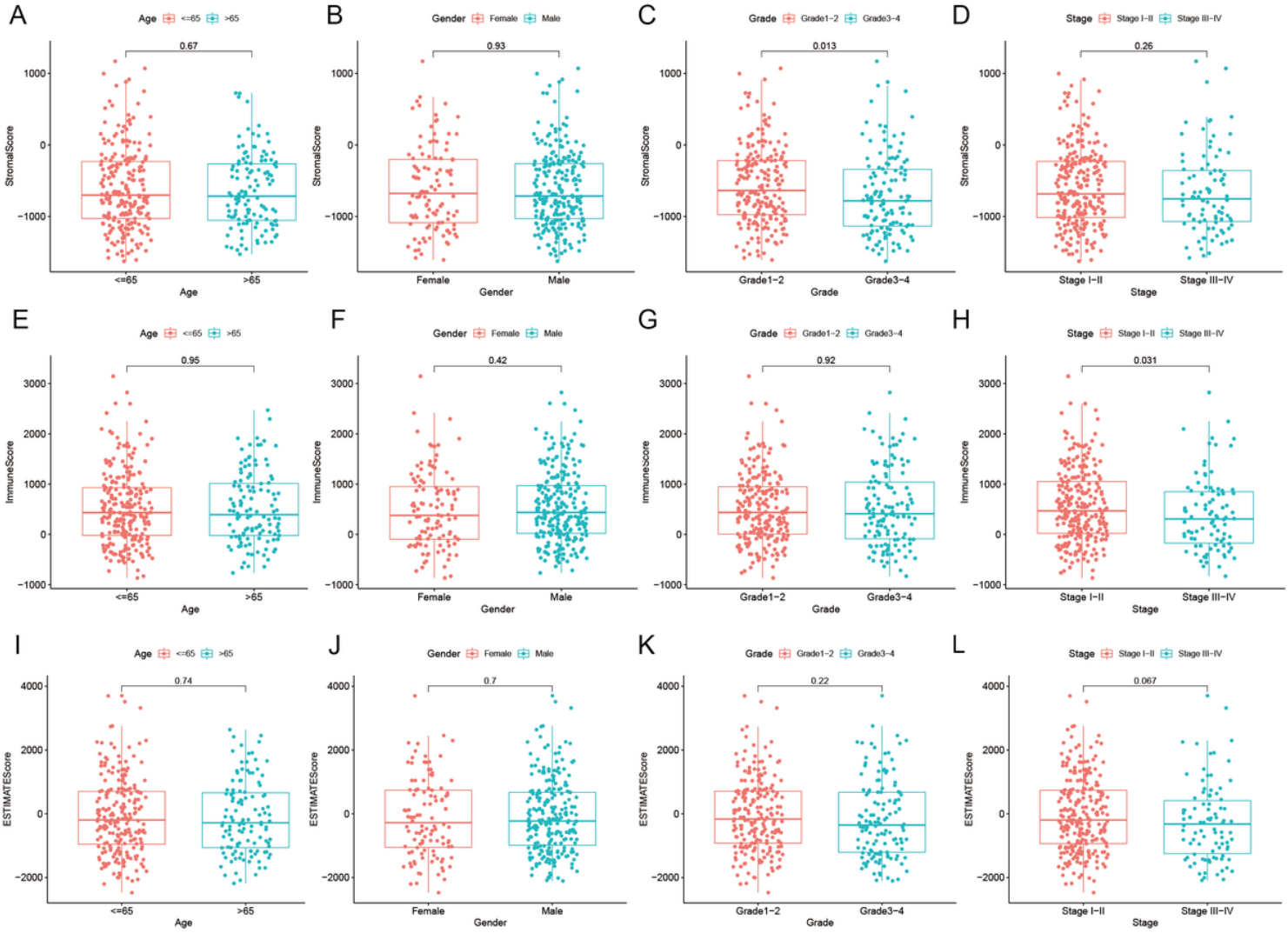

Figure 3

The relationship of immune/stromal/Estimate/scores with different clinicopathologic parameters of HCC patients. (A-D) The association of stromal scores with different Age groups (<=65 and >65), Gender groups (Female and Male), Grade groups (Grade I-II and Grade III-IV), Stage groups (Stage I-II and Stage III-IV). (E-H) The association of immune scores with different Age groups (<=65 and >65), Gender groups (Female and Male), Grade groups (Grade I-II and Grade III-IV), Stage groups (Stage I-II and Stage III-IV). (I-L) The association of ESTIMATE scores with different Age groups (<=65 and >65), Gender groups (Female and Male), Grade groups (Grade I-II and Grade III-IV), Stage groups (Stage I-II and Stage III-IV).

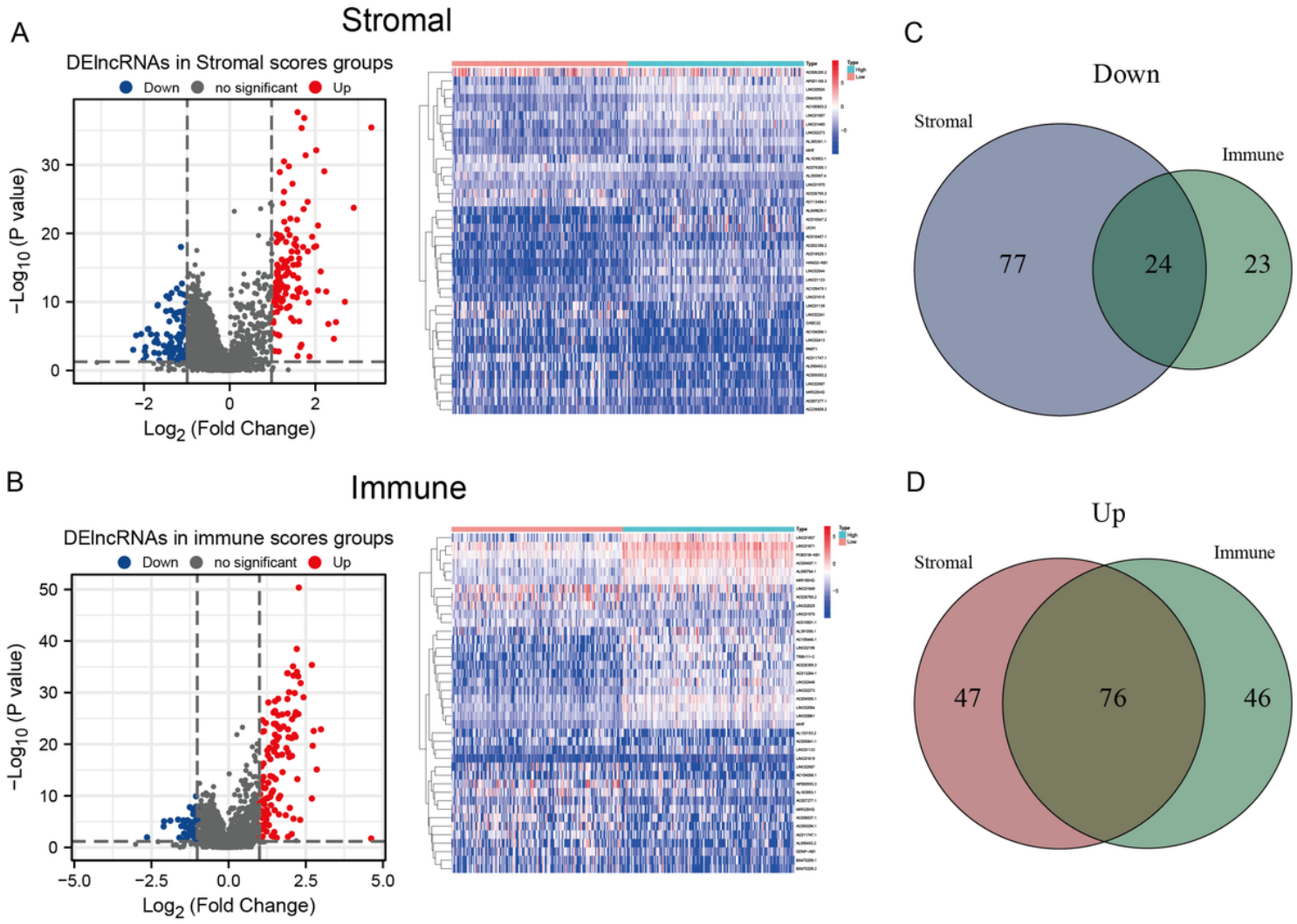

Figure 4

DElncRNAs between high- and low- stromal/immune scores groups. (A) The volcano plot and heatmap of DElncRNAs in high- and low-stromal scores groups. (B) The volcano plot and heatmap of DElncRNAs in high- and low-immune scores groups. (C) The downregulated lncRNAs in both stromal score and immune scores groups by Venn diagram. (D) The upregulated lncRNAs in both stromal score and immune scores groups by Venn diagram.

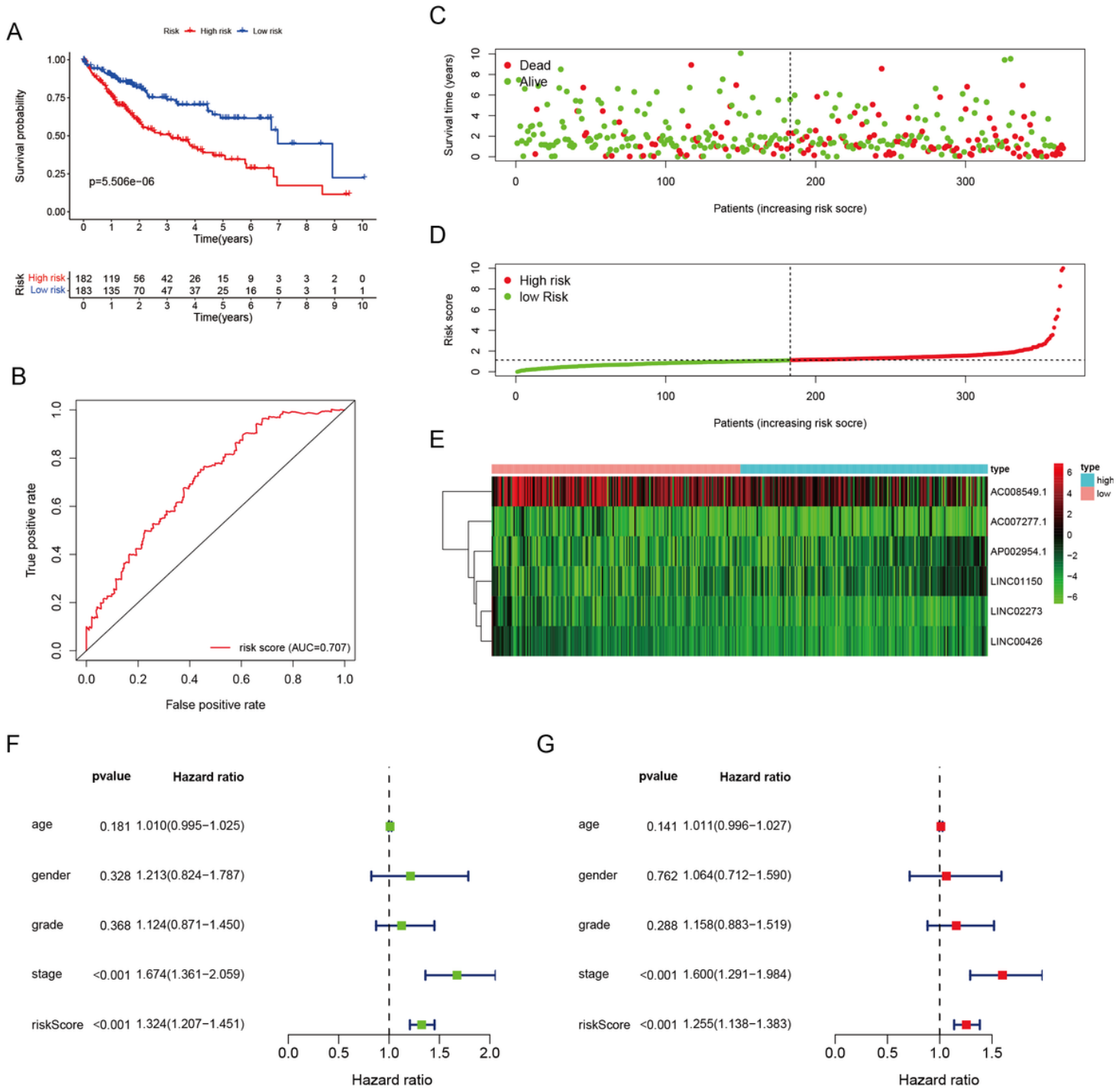

Figure 5

Construction and validation of the TME-related lncRNAs signature in HCC samples. (A) Kaplan-Meier survival analysis of the high-risk and low-risk groups. (B): Receiver operating characteristic (ROC) curve evaluated predictive accuracy of the prognostic model. (C) The risk scores curves based on the risk score of each HCC patient. (D) The scatter plots display the survival status of each HCC patient. (E): The heatmap exhibit the expression levels of the six TME-related lncRNAs in the high-risk and low-risk groups. (F) Univariate Cox regression analysis of clinical features and risk score in HCC samples. (G) Multivariate Cox regression analysis of clinical features and risk score in HCC samples.

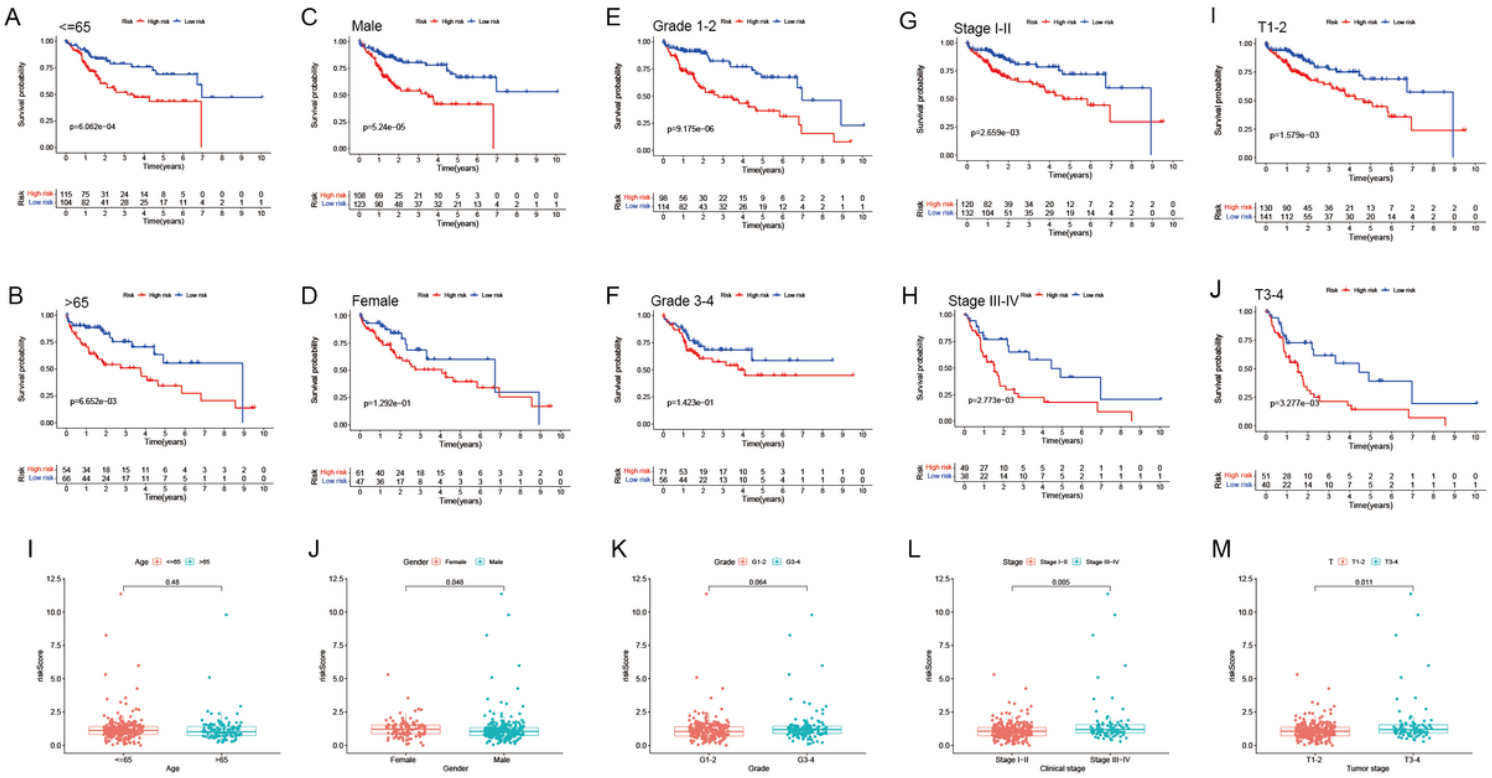

Figure 6

Subgroup analysis the correlation of clinical features with risk signature. (A-J) Kaplan-Meier survival curves analysis of risk group with Age subgroups (<=65 and >65), Gender subgroups (Female and Male), Grade subgroups (Grade I-II and Grade III-IV), Stage subgroups (Stage I-II and Stage III-IV), Tumor stage subgroups (T1-2 and T3-4). (I-M) The differential analysis of risk scores in different subgroup with Student's t-test or rank-sum test.

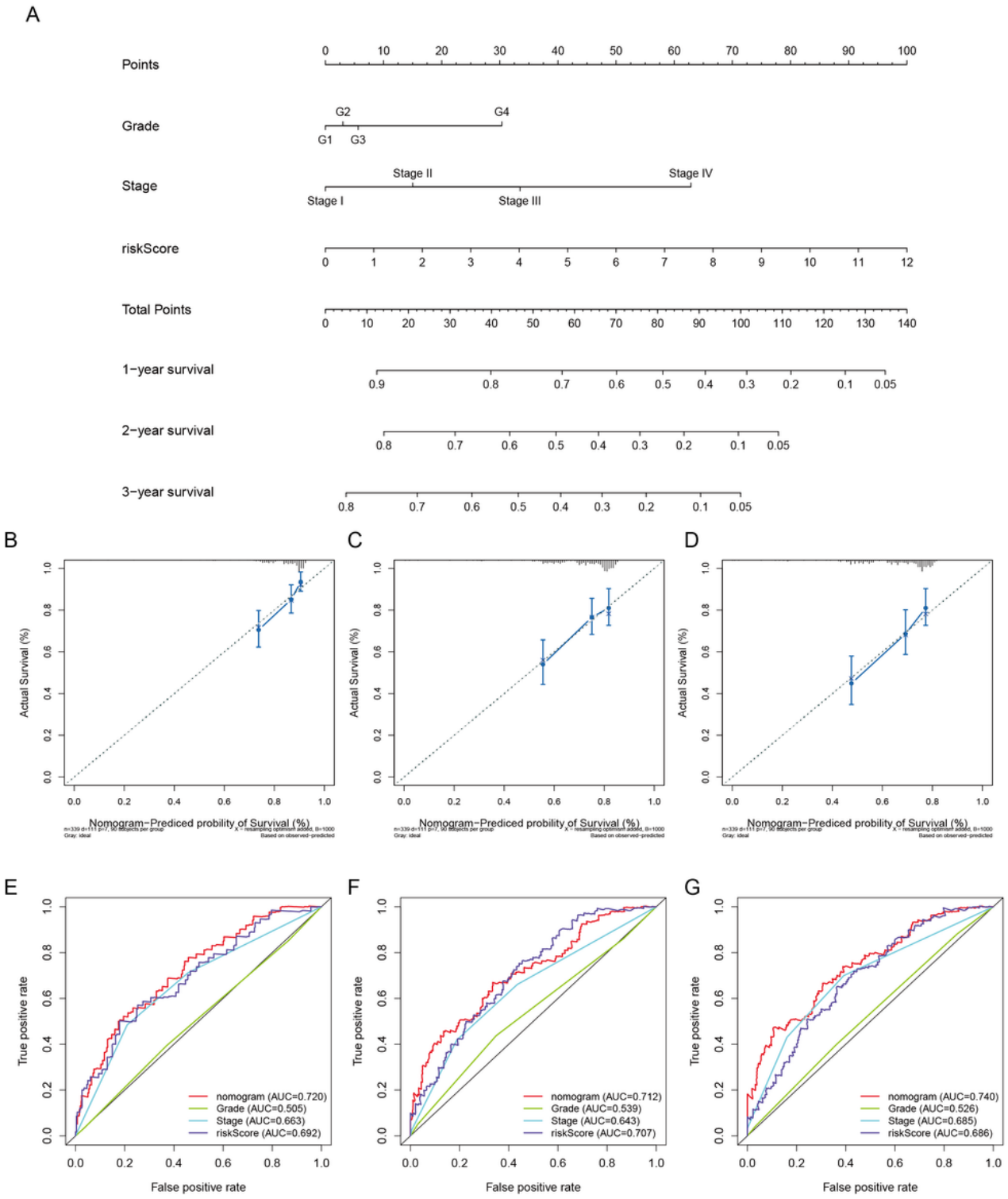

Figure 7

The construction of the predictive nomogram for HCC patients from TCGA. (A) Nomogram predicting the probability of 1-, 2- and 3-year OS for HCC patients. (B-D) Calibration curve showed the predictive accuracy of the nomogram. The Y-axis represents actual survival, and the X-axis represents nomogram-predicted survival. (E-G) The ROC curves analysis assessed the prediction performance of the nomogram for 1-, 2-and 3-year OS.

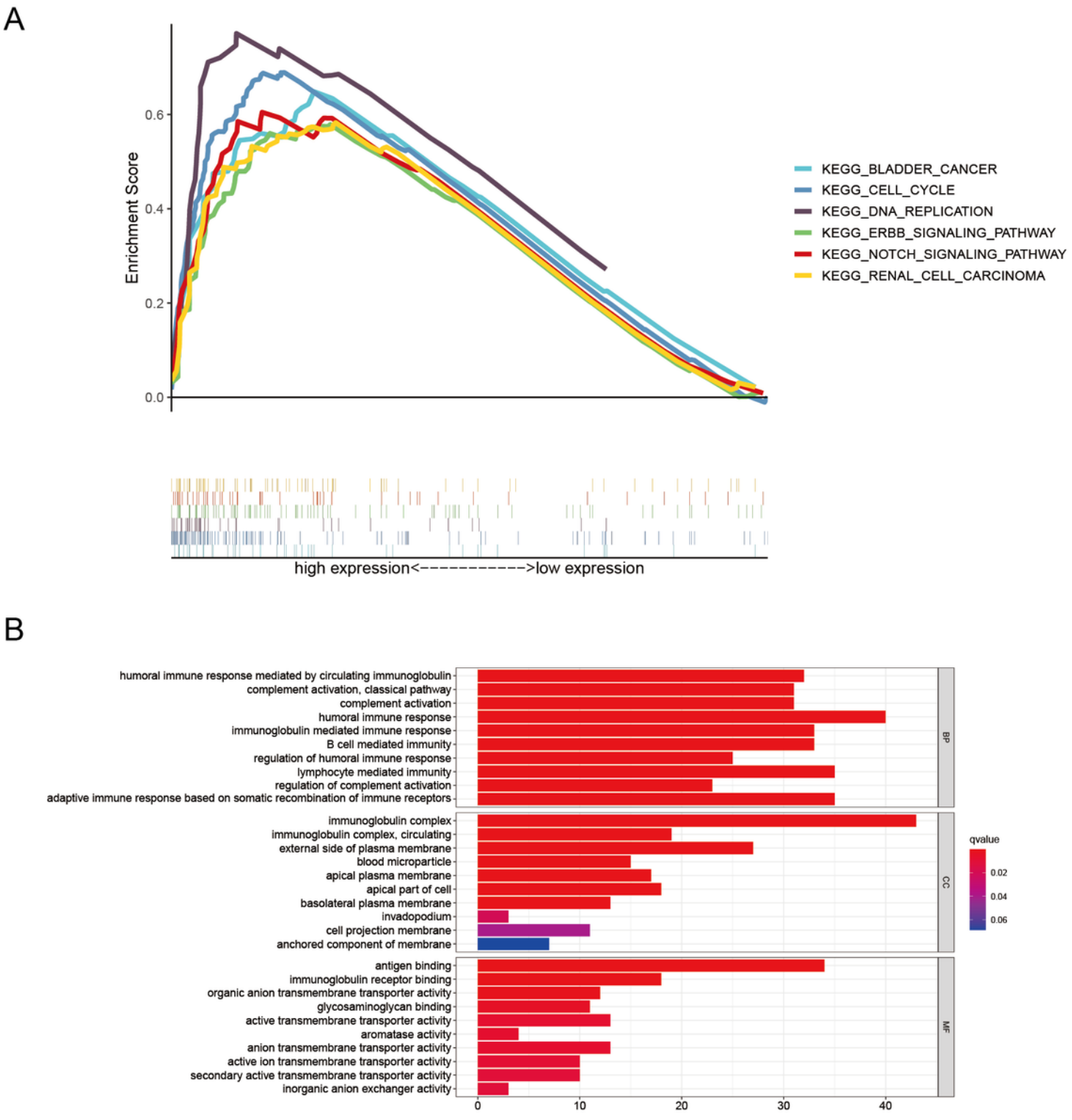

Figure 8

Functional enrichment analysis of the low- and high-risk group. (A) Gene set enrichment analysis (GSEA) based on risk grouping in the cohort from TCGA. (B) Gene Ontology (GO) analysis of the differentially expressed genes (DEGs) basing on high and low-risk groups.

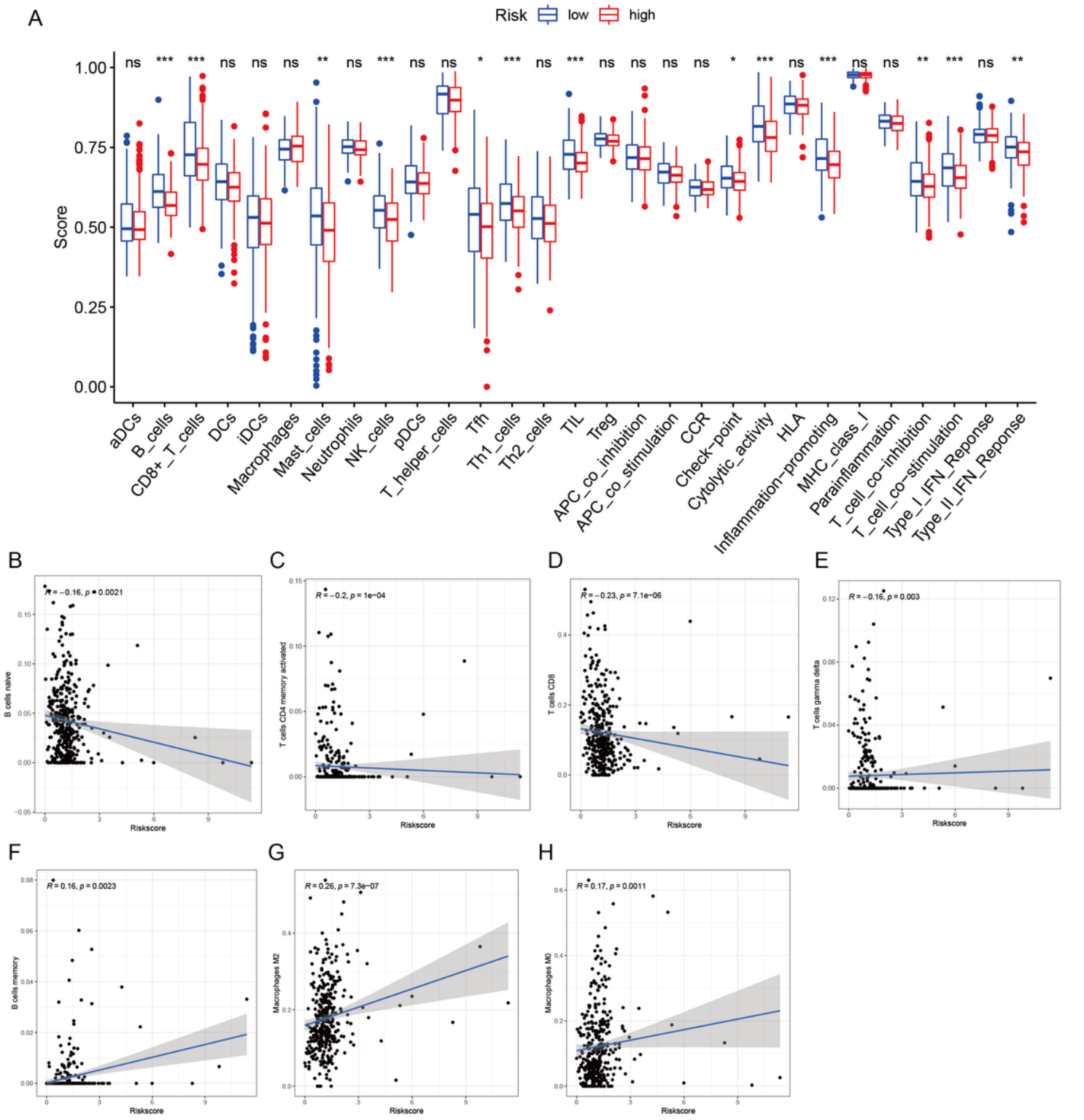

Figure 9

Tumor Immune microenvironment states analysis of the TME-related lncRNAs signature based on ssGSEA and CIBERSORT algorithm. (A) Comparison of the immune cells infiltration and immune functions between low- and high-risk groups. (B-H) Correlation analysis between immune cells infiltration levels and risk score. *P< 0.05; **P< 0.01; ***P< 0.001. ssGSEA: single-sample gene set enrichment analysis

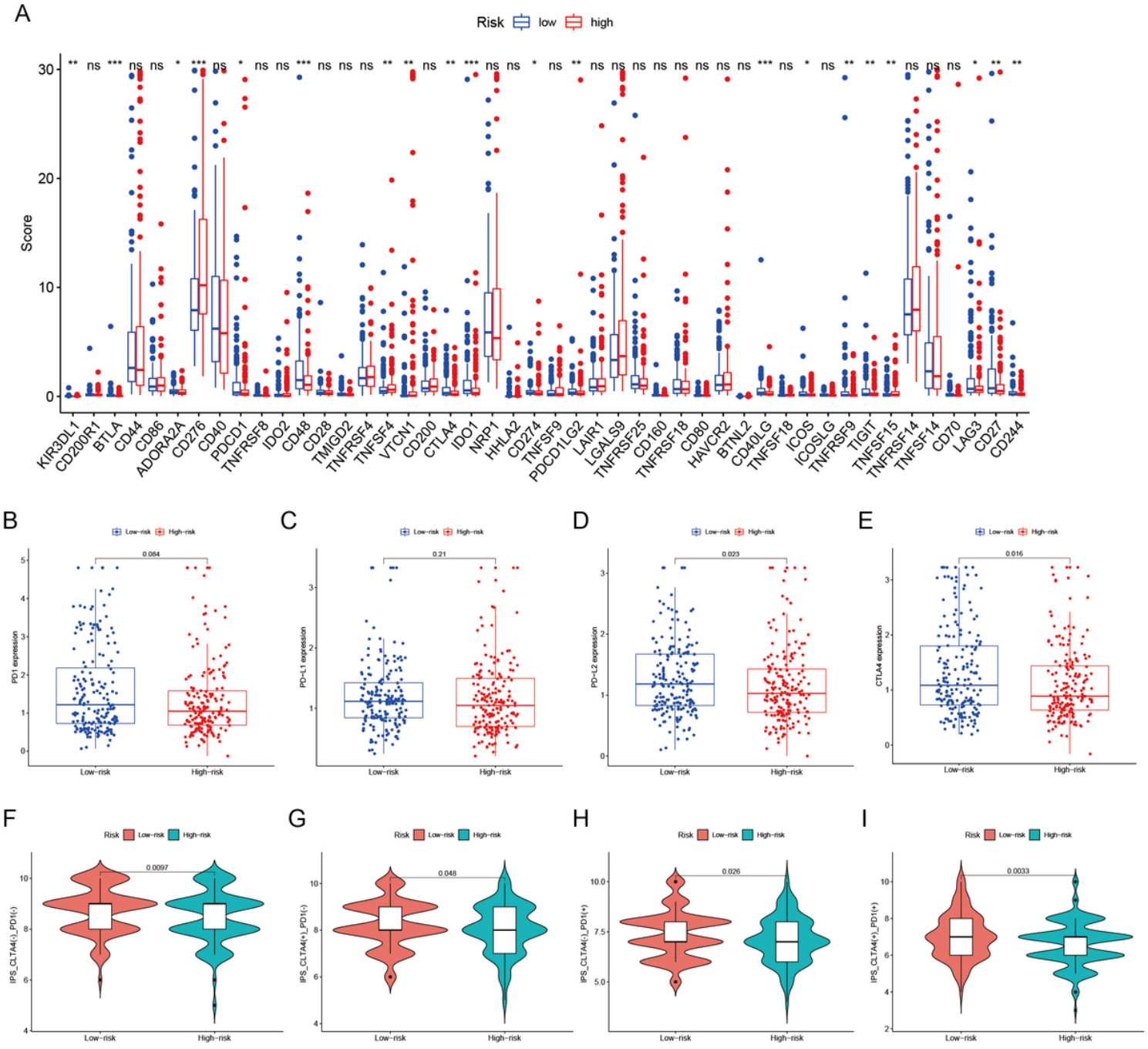

Figure 10

The correlation of TME-related lncRNAs signature with ICBs-related genes and treatment response to ICBs. (A) Comparison of 46 immune checkpoint blockade–related genes expression levels in high- and low-risk score subgroups. (B-E) The difference of the expression level of PD-1,PD-L1,PD-L2, and CTLA4 between high- and low-risk groups. (F-I) Comparison of treatment response of ICBs in two risk score subgroups. ICBs: Immune checkpoint inhibitors.

Supplementary Files

This is a list of supplementary files associated with this preprint. Click to download.

- renamed94b1c.docx
- renamedcb09e.docx
- renamedd6b0c.docx
- renamed70d66.docx